TU/e EINDHOVEN UNIVERSITY OF TECHNOLOGY

Run flat tires versus conventional tires

Citation for published version (APA):
Veld, op het, I. B. A. (2006). *Run flat tires versus conventional tires: an experimental comparison*. (DCT rapporten; Vol. 2006.042). Technische Universiteit Eindhoven.

Document status and date:
Published: 01/01/2006

Document Version:
Publisher's PDF, also known as Version of Record (includes final page, issue and volume numbers)

Please check the document version of this publication:

• A submitted manuscript is the version of the article upon submission and before peer-review. There can be important differences between the submitted version and the official published version of record. People interested in the research are advised to contact the author for the final version of the publication, or visit the DOI to the publisher's website.
• The final author version and the galley proof are versions of the publication after peer review.
• The final published version features the final layout of the paper including the volume, issue and page numbers.

Link to publication

General rights
Copyright and moral rights for the publications made accessible in the public portal are retained by the authors and/or other copyright owners and it is a condition of accessing publications that users recognise and abide by the legal requirements associated with these rights.

• Users may download and print one copy of any publication from the public portal for the purpose of private study or research.
• You may not further distribute the material or use it for any profit-making activity or commercial gain
• You may freely distribute the URL identifying the publication in the public portal.

If the publication is distributed under the terms of Article 25fa of the Dutch Copyright Act, indicated by the "Taverne" license above, please follow below link for the End User Agreement:

www.tue.nl/taverne

Take down policy
If you believe that this document breaches copyright please contact us at:

openaccess@tue.nl

providing details and we will investigate your claim.

Download date: 04. Oct. 2023

Run Flat Tires
vs.
Conventional Tires
An Experimental Comparison

I.B.A. op het Veld
DCT 2006.042

Internal Traineeship

Supervisors: Dr. Ir. A.J.C. Schmeitz
Dr. Ir. I.J.M. Besselink
Prof. Dr. H. Nijmeijer

Eindhoven University of Technology
Department Mechanical Engineering
Dynamics and Control Technology Group

Eindhoven, May 2006

Summary

Run Flat Tires vs. Conventional Tires, an Experimental Comparison – I.B.A. op het Veld

Tires play an important role in comfort, handling and safety of a vehicle. They are the key link in the force transmission between the road and the vehicle. During their lifetime tires are exposed to many different road and environmental conditions. Most flat tires are the result of (slow) leaks that go unnoticed and allow the tire's air pressure to drop. This pressure drop has serious consequences for the comfort, handling and safety of a vehicle. One of the technologies used to help maintain vehicle mobility when a tire is punctured, are self-supporting tires (so called Run Flat Tires).

In this study, an experimental comparison is carried out between Run Flat Tires and conventional tires. Run Flat Tires feature a stiffer internal construction compared with conventional tires. This has an effect on the handling behavior and the ride comfort. The subject of this research project is the study of the characteristic differences of conventional tires and Run Flat Tires. The aims of this research are: (1) examination of the characterizations of conventional tires and Run Flat Tires and (2) understanding the differences in characterizations between conventional tires and Run Flat Tires.

To achieve these aims, a number of experiments are carried out on the Tire Flat Plank Test Facility of Eindhoven University of Technology and analyzed to create a better perception of the characterization differences. The following characterization areas are examined: (i) the effective rolling radius, (ii) the lateral and vertical stiffness, (iii) the sideslip relaxation and (iv) the enveloping behavior. This report deals with the outcome of these experiments and describes the differences in characterizations.

The results of the experiments show: (i) the difference between the effective rolling radius of run flat tires and conventional tires is minimal; (ii) the lateral stiffness of run flat tires is considerably higher than that of conventional tires (up to 50 percent). Above a vertical load of 3 kN the vertical stiffness of the run flat tires increases significantly more progressively; (iii) the relaxation lengths of run flat tires and conventional tires do not significantly differ; (iv) The enveloping behavior at constant vertical load is very similar; at constant axle height the enveloping behavior is quite different, i.e. the vertical forces for the run flat tires are much higher.

For further research, it is suggested to repeat the enveloping experiments for the other run flat (Bridgestone) and conventional tire (Dunlop). Furthermore, it is interesting to carry out additional measurements to completely characterize the run flat tires. For further research this would mean: principal tire modes, damping ratios, slip characteristics, vertical stiffness at various velocities, etc. To investigate the differences between run flat and conventional tires with respect to for example ride comfort, vehicle simulations and measurements have to be carried out on various road surfaces. This, because when a vehicle drives over an uneven road surface the axle height is not constant and also the vertical load is not constant, which means that the current measurements cannot directly give a clear answer.

Samenvatting

Run Flat Banden versus Conventionele Banden, een Experimenteel Vergelijk – I.B.A. op het Veld

Banden spelen een belangrijke rol in het comfort, het weggedrag en de veiligheid van een voertuig. Bij de krachtoverdracht tussen wegdek en voertuig zijn banden dé koppeling. Tijdens hun levensduur worden banden blootgesteld aan verschillende wegdek- en omgevingscondities. Veel platte banden zijn het resultaat van (kleine) lekkages die onopgemerkt blijven en ervoor zorgen dat de luchtdruk in de band daalt. Deze daling van de bandenspanning heeft ernstige gevolgen voor het comfort, het weggedrag en de veiligheid van een voertuig. Eén van de technologieën die gebruikt wordt om de voertuigmobiliteit te waarborgen als een band lek raakt, zijn zelfondersteunende banden (zogenaamde Run Flat Banden).

In deze studie wordt een experimenteel vergelijk gemaakt tussen Run Flat Banden en Conventionele Banden. Run flat banden bezitten, in vergelijking met conventionele banden, een stijvere interne constructie. Deze stijvere interne constructie heeft invloed op het weggedrag en het rijcomfort van een voertuig. Het onderwerp van dit onderzoeksproject is het onderzoeken van de karakteristieke verschillen tussen run flat banden en conventionele banden. De doelstellingen van dit onderzoek zijn: (1) het bestuderen van de karakteristieke eigenschappen van conventionele en run flat banden en (2) het begrijpen van de karakteristieke verschillen tussen run flat banden en conventionele banden.

Om deze doelstellingen te verwezenlijken, zijn een aantal experimenten uitgevoerd met de Tire Flat Plank Test Faciliteit van de Technische Universiteit Eindhoven en geanalyseerd om een beter inzicht te krijgen in de karakteristieke verschillen. De onderzochte karakteristieke eigenschappen zijn: (i) de effectieve rolstraal, (ii) de laterale en verticale stijfheid, (iii) de slip relaxatie en (iv) het 'enveloping'-gedrag. De resultaten van deze experimenten en de verschillen in karakteristieke eigenschappen worden in dit rapport beschreven.

De resultaten van de experimenten laten het volgende zien: (i) het verschil tussen de effectieve rolstraal van run flat banden en conventionele banden is minimaal, (ii) de laterale stijfheid van run flat banden is aanzienlijk hoger dan die van conventionele banden (tot 50 procent hoger). Boven een verticale belasting van 3 kN neemt de verticale stijfheid van run flat banden significant progressiever toe dan bij conventionele banden. (iii) de relaxatie lengte van run flat en conventionele banden verschillen nauwelijks van elkaar (iv) het 'enveloping-gedrag' bij constante verticale belasting is vrijwel gelijk; bij constante ashoogte is er een groot verschil in 'enveloping'-gedrag, d.w.z. de verticale krachten voor run flat banden zijn veel hoger.

Voor verder onderzoek wordt voorgesteld de 'enveloping' experimenten uit te voeren voor de andere run flat (Bridgestone) en conventionele band (Dunlop). Verder is het interessant om extra experimenten uit te voeren om de run flat banden volledig te karakteriseren. Voor verder onderzoek betekent dit: voornaamste band trilvormen, demping ratio's, slip karakteristieken, verticale stijfheid bij verschillende snelheden, etc. Tot slot is het interessant om voertuigsimulaties en experimenten uit te voeren ten aanzien van bijvoorbeeld het rijcomfort op verschillende wegdekken. Dit aangezien een voertuig rijdend over een oneffen weg, geen constante ashoogte en verticale belasting heeft en er met de huidig uitgevoerde experimenten geen direct duidelijk antwoord kan worden gegeven ten aanzien van bijvoorbeeld het rijcomfort.

Table of contents

Summary **2**
Samenvatting **3**
List of Symbols **5**
1 Introduction **6**
1.1 Motivation and background 6
1.2 Aim and scope 7
1.3 Contents of the report 7
2 Carried out experiments **8**
2.1 Flat plank tire test facility 8
2.2 Pre-measuring actions 9
2.3 Effective rolling radius 10
2.4 Stiffness measurements 11
2.4.1 Vertical stiffness 11
2.4.2 Lateral stiffness 11
2.5 Sideslip relaxation 12
2.6 Cleat measurements 13
2.6.1 Step obstacle 13
2.6.2 Sine obstacle 14
3 Discussion of the measuring results **15**
3.1 Effective rolling radius 15
3.2 Stiffness measurements 17
3.2.1 Vertical stiffness 17
3.2.2 Lateral stiffness 18
3.3 Sideslip relaxation 20
3.4 Enveloping behavior 22
3.4.1 Step obstacle 22
3.4.2 Sine obstacle 26
4 Conclusions and Recommendations **27**
4.1 Conclusions 27
4.2 Recommendations 28
References **29**
Appendix 1 Forces and moments transformation **30**
Appendix 2 Vertical stiffness **32**
A2.1 Vertical stiffness (non-rolling situation) 32
A2.2 Vertical stiffness polynomial fits 33
Appendix 3 Contact length **37**
Appendix 4 Measurement file name explanation **40**

List of Symbols

Symbol	Unit	Description
a	m	distance between strain gauges
b	m	distance between G_{x2} and wheel centre plane
$C_{F\alpha}$	N/rad	cornering stiffness
C_{Fy}	N/m	lateral stiffness
C_{Fz}	N/m	vertical stiffness
dy	m	lateral tire deflection
dz	m	vertical deflection
f_{sample}	Hz	sample frequency data acquisition system
F_{ax}	N	longitudinal component of measuring hub force
F_{az}	N	vertical component of measuring hub force
F_{azo}	N	initial vertical component of measuring hub force
F_x	N	longitudinal force
F_y	N	lateral force
$F_{y,so}$	N	steady state lateral force
F_z	N	vertical force
G_{x1} and G_{x2}	N	longitudinal force strain gauges
G_y	N	lateral force strain gauges
G_{z1} and G_{z2}	N	vertical force strain gauges
K_x	N	longitudinal force at wheel centre
K_y	N	lateral force at wheel centre
K_z	N	vertical force at wheel centre
l_s	m	contact length
M_x	Nm	moment about x-axis at contact plane
M_y	Nm	moment about y-axis at contact plane
M_z	Nm	moment about z-axis at contact plane
N	-	number of samples
r	m	loaded tire radius
r_e	m	effective rolling radius
r_f	m	free tire radius
T_x	Nm	moment about x-axis at wheel centre
T_y	Nm	moment about y-axis at wheel centre
T_z	Nm	moment about z-axis at wheel centre
V_x	m/s	forward velocity
w	m	effective road height
w_c	m	road height correction
α	deg	side slip angle
β_y	deg	effective forward slope
γ	deg	camber angle
μ	-	lateral friction coefficient
ρ	m	radial tire deflection
Ω	rad/s	angular velocity
σ_α	m	side slip relaxation length

1 Introduction

The first chapter gives an introduction concerning the work described in this report. Motivation, background, aim and the scope of this project are presented. Furthermore a brief outline of the contents of the report is given.

1.1 Motivation and background

Tires play an important role in comfort, handling and safety of a vehicle. During their lifetime tires are exposed to many different road and environmental conditions.
There are basically three elements of a tire which determine the load capacity of the tire and maintain the contact patch: the size of the air chamber between the tire and the rim, the strength provided by the tire construction and the amount of air pressure in the tire. Most flat tires are the result of (slow) leaks that go unnoticed and allow the tire's air pressure to drop.
There are three technologies used to help maintain vehicle mobility when a tire is punctured. These are self-sealing tires, tires supported by an auxiliary system and self-supporting tires (so called Run Flat Tires). Self-sealing tires are designed to fix most tread-area punctures instantly and permanently. In Auxiliary supported systems, the flat tire's tread rests on a support ring attached to the wheel when the tire loses pressure [4]. Run Flat Tires feature a stiffer internal construction. These kinds of tires are used during experiments in this project. Run Flat Tires are capable of temporarily carrying the weight of the vehicle, even after a tire has lost all air pressure.
To provide "self-supporting" capability, there are rubber inserts attached next to or between layers of heat-resistant cord in the sidewalls to help prevent breaking the reinforcing cords if air pressure is lost, (Fig. 1.1). They also feature specialized beads that allow the tire to firmly grip the rim even in the event of air loss.
In practice, run flat tires can operate with 80 km/h for 80 km in the event of air loss [6].

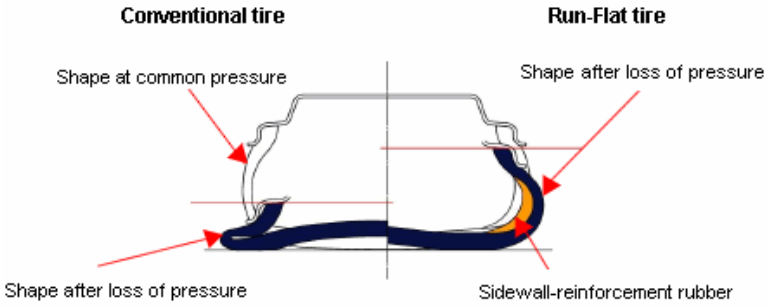

Fig. 1.1, S*idewall distortion conventional tire and run flat tire [5]*

1.2 Aim and scope

Run Flat Tires feature a stiffer internal construction compared with conventional tires. This stiffer internal construction has an effect on the handling behavior and the ride comfort. The study of the characteristic differences of conventional tires and Run Flat Tires is the subject of the research project described in this report.

The aims of this research project are:

- Examining the characterizations of conventional tires and Run Flat Tires.
- Understanding the differences in characterizations between conventional tires and Run Flat Tires.

To achieve these aims, a number of experiments have been carried out on the Tire Flat Plank and analyzed to create a better perception of the characterization differences. Tires are tested in a quasi-static way (meaning: very low speed) to eliminate any dynamic influences on the characterizations. The experiments as well as the outcome of the experiments will be described in this report.

1.3 Contents of the report

The outline of this report is as follows. Chapter 2 describes the experiments that are carried out with the Tire Flat Plank. In addition, the Flat Plank facility, the used tires and pre-measuring activities are discussed.

The measuring results are subject of discussion of Chapter 3. The results of the different experiments are presented and explained. Furthermore, the differences in characterizations are discussed.

Finally, in Chapter 4 the research and the conclusions are summarized and recommendations for further research are formulated.

2 Carried out experiments

In this Chapter first the tire test facility used to carry out the experiments is described and after that pre-measuring actions taken will be explained. Finally, the experiments and experimental conditions will be discussed.

2.1 Flat plank tire test facility

The Flat Plank can perform measurements for combined slip characteristics, relaxation lengths and tire response on road irregularities.

The Flat Plank Tire Tester, Figure 2.1, consists of a flat steel road surface (flat plank), measuring hub, turn table and axle height, lateral position and camber adjust mechanism. The flat plank is positioned upside down and can be moved with a constant speed. To create a slip angle, the tire attached on the measuring hub can be turned around the vertical axis on the turn table. The measuring hub can be moved in lateral direction to change the lateral position of the tyre compared to the flat plank. The axle height can be adjusted by a jack (constant axle height) or by an air spring system (constant vertical load). The camber angle can be adjusted by rotating the flat plank around the axis on its surface and by rotating the measuring hub around its longitudinal axis. Different obstacles (cleats) with a maximum height of 30 mm can be mounted on the flat plank to create road irregularities.

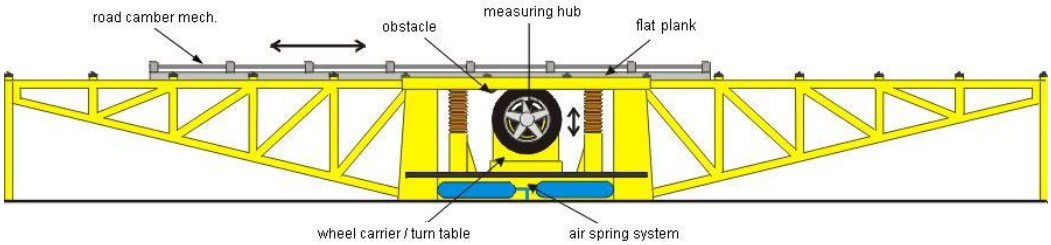

Fig. 2.1, *Flat Plank Tire Tester [3]*

The flat plank speed can vary between 0 and 4.75 cm/s. The measuring hub can measure reaction forces and moments in the wheel axle. The following forces and moments are measured: longitudinal force (F_x), lateral force (F_y), vertical force (F_z), overturning moment (M_x) and aligning moment (M_z) (see Appendix 1). The measuring hub can measure reaction forces (up to 10 kN) and moments by using five strain gauge bridges. The rotation angle and rotation velocity of the wheel and the displacement and velocity of the flat plank are measured with incremental encoders. Furthermore, the slip angle and vertical displacement of the measuring hub are measured.

The measured signals are sent to the signal conditioning system. This system contains an amplifier, power supply, lowpass filter and an A/D converter. After A/D conversion, the data is sampled by a data acquisition program (LABView). The sampling starts by a triggering signal.

2.2 Pre-measuring actions

In order to have reproducible experiments a number of pre-measuring actions have to be done before experiments start. The different measurements are saved with a unique name containing measurement identification, vertical load and tire code.

Start positioning
Every experiment is performed three times under the same conditions, meaning: axle height and vertical load. Each tire has three different start measuring positions, while starting each time at the same position on the flat plank (Fig. 2.3).

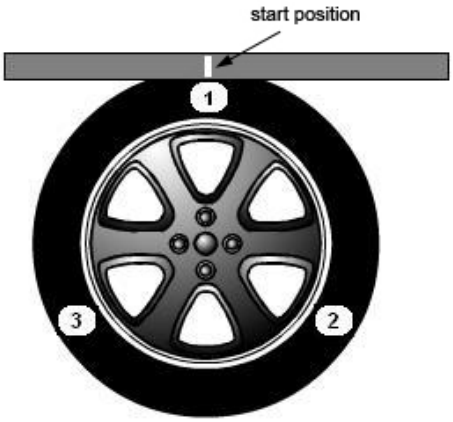

Fig. 2.3, *Start positions tire and flat plank*

Reference measurements
Tires usually produce side force and aligning torque, even in traveling at zero slip angle and zero camber angle, because of the effects: *ply-steer* and *conicity*. Furthermore, the forces and moments vary when traveling due to non-uniformities in the tire structure. Reference measurements have to be carried out to minimize the influence of these phenomena on the processed data. Corrected data is obtained by subtracting the reference measurement data from the raw experiment data. To correctly eliminate ply-steer and conicity for a certain angular position of the tire and the longitudinal position of the flat plank, the markers on the tire and the flat plank should coincide with each other before the measurement starts.

For the experiments, the following tires are used:

Code	Tire	Dimensions	Inflation pressure
GE	Goodyear Eagle NCT5 EMT	205/55 R16	2.3 bar
BT	Bridgestone Turanza RFT	205/55 R16	2.3 bar
DS	Dunlop SP Sport 2000*E	225/50 R16	2.3 bar
MP	Michelin Pilot HX	205/55 R16	2.3 bar

Table 2.1, *Tires used in experiments.*

The Goodyear Eagle and Bridgestone Turanza are tires with run flat technology. All tires are mounted on the same type of rim with an ET value of 34 mm, except the Goodyear Eagle has an ET value of 20 mm. The code indications are used to identify the different tires during measuring and post processing.

2.3 Effective rolling radius

The effective rolling radius (r_e) is defined as the ratio of the forward velocity (V_x) and the angular velocity (Ω) of the freely (no brake or drive torque is applied; V_{sx}=0 tire.

$$r_e = \frac{V_x}{\Omega} \tag{2.1}$$

This is illustrated in Fig. 2.4.

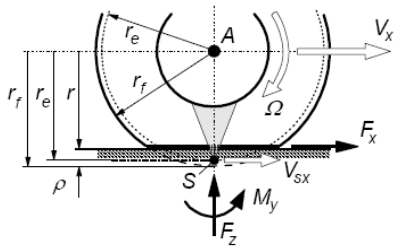

Fig. 2.4, *Effective rolling radius [1]*

In the figure, r_f and r represent the free tire radius (or unloaded radius) and the loaded tire radius respectively. The radial deflection (ρ) is defined as the reduction of the unloaded tire radius to the loaded tire radius.

$$\rho = r_f - r \tag{2.2}$$

The effective rolling radius depends on the vertical load. Therefore the measurements are carried out for different vertical loads, see Table 2.1:

Vertical load [kN]
1
2
3
4
5
6

Table 2.1, *Vertical load cases*

Measurement procedure

(1) Press the tire vertically against the flat plank until desired vertical load is reached (at constant axle height)

(2) Start the flat plank (constant speed: 4.75 cm/s)

During (2) data is sampled (with: f_{sample} = 50 Hz, N = 2500 data points).

2.4 Stiffness measurements

The stiffness experiments are carried out to determine the vertical stiffness and the lateral stiffness of the tires.

2.4.1 Vertical stiffness

In general, the vertical stiffness (C_{Fz}) is defined as the derivative of the vertical force (F_z) and the vertical tire deflection (ρ).

$$C_{F_z} = \frac{\partial F_z}{\partial \rho} \tag{2.3}$$

Measurement procedure

(1) Place the tire vertically against the flat plank
(2) Start the plank
(3) Raise vertical load, with constant speed, till 9 kN
(4) Lower vertical load, with constant speed, till 0 kN
(5) Save measurement with unique filename

The measurements are carried out for both a rolling and static (stand still) situation.
For the measurements in static situation, (2) is skipped.
From step (3) data is sampled (with: f_{sample} = 25 Hz, N = 2500 data points).

2.4.2 Lateral stiffness

In general, the lateral stiffness is defined as the derivative of the lateral force (F_y) versus the lateral tire deflection (dy). Here, the lateral stiffness (C_{Fy}) represents the slope of the linear section of the function $F_y(dy)$

$$C_{F_y} = \left.\frac{\partial F_y}{\partial dy}\right|_{dy=0} \tag{2.4}$$

Measurement are carried out for different vertical loads, see Table 2.2:

Vertical load [kN]
2
4
6

Table 2.2, *Vertical load cases*

Measurement procedure

(1) Apply turn angle of 90 degree
(2) Press the tire vertically against the flat plank until desired vertical load is reached (at constant axle height)
(3) Start the flat plank (small displacement)

During (3) data is sampled (with: f_{sample} = 100 Hz, N = 300 data points).

2.5 Sideslip relaxation

The sideslip relaxation length (σ_α) is defined as the length that corresponds with 63 percent of the steady-state lateral force level, see figure 2.5.

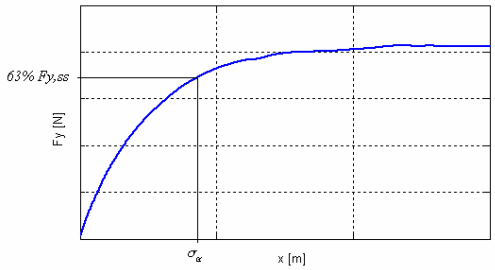

Fig. 2.5, *Sideslip relaxation length*

The measurements are carried out with a sideslip angle (α) of 1 degree. For small slip angles it is valid to linearize the force and moment characteristics. The lateral force can be represented by the following expression:

$$F_y = C_{F\alpha}\alpha \tag{2.5}$$

where ($C_{F\alpha}$) is the cornering stiffness. This expression is valid for small pure sideslip angles, and without the effect of camber.

Measurements are carried out for the different vertical loads and slip angles, see Table 2.3.

Vertical load [kN]	Sideslip angle [deg]
2	0
4	
6	
2	1
4	
6	

Table 2.3, *Vertical load and slip angle cases*

Measurement procedure

(1) Apply desired sideslip angle
(2) Press the tire vertically against the flat plank until desired vertical load is reached (at constant axle height)
(3) Start the flat plank (constant speed: 4.75 cm/s)

During (3) data is sampled (with: f_{sample} = 50 Hz, N = 2500-3000 data points).
The measurements with sideslip angle 0 degree represent the reference measurements.

2.6 Cleat measurements

In order to evaluate the enveloping behavior, the response of the tire rolling over an obstacle will be measured. The obstacle shapes used for the measurements are a step and sine.

2.6.1 Step obstacle

Measurements are carried out with three different step heights, namely 10, 20 and 30 mm. The step obstacle is created by mounting one or more 10 mm aluminium plates on the flat track. The cross-sections are depicted in Fig. 2.6.

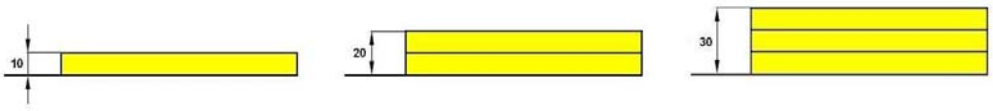

Fig. 2.6, *Cross sections of step obstacles used for cleat measurements*

For measurements, the vertical load cases are applied as depicted in Table 2.4.

Vertical load [kN]	Step height [mm]
2	10
4	
6	
2	20
4	
6	
2	30
4	
6	

Table 2.4, *Vertical load cases*

The step obstacle measurements are carried out with constant vertical load instead of constant axle height. The flat plank speed is reduced from 4.75 cm/s to 2.38 cm/s.

Measurement procedure

(1) Mount the desired cleat on the flat plank
(2) Determine the longitudinal distance from the trigger position to the position at which the edge of the step is vertically in line with the wheel centre. (this is only done once)
(3) Place tire and flat plank back in the starting/trigger position

(4) Press the tire vertically against the flat plank until the desired vertical load is reached (at constant vertical load)
(5) Start the flat plank

During (5) data is sampled. (with: f_{sample} = 50 Hz, N = 1250 data points)
The reference measurements are done skipping (1) and (2).

2.6.2 Sine obstacle

The sine obstacle is created by mounting first the sine obstacle to a 10 mm aluminium plate (step obstacle) and then mounting this plate with sine obstacle on the flat plank. Like the step obstacle, the sine obstacle is manufactured of aluminium.
The cross section is depicted in Fig. 2.7.

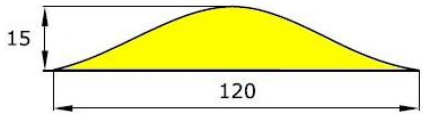

Fig. 2.7, *Cross section of sine obstacle used for cleat measurements*

The measurements are carried out for different vertical loads, see Table 2.5.

Vertical load [kN]
2
4
6

Table 2.5, *Vertical load cases*

The sine obstacle measurements are carried out with constant axle height in order to investigate the influence of the vertical stiffness on the enveloping behavior. The track speed is reduced from 4.75 cm/s to 2.38 cm/s.

Measurement procedure
(1) Mount plate with sine obstacle to the flat plank
(2) Position the wheel centre at the start of the plate
(3) Press the tire vertically against the flat plank until desired vertical load is reached (at constant axle height)
(4) Start the flat plank

During (4) data is sampled (with: f_{sample} = 50 Hz, N = 1750 data points).
The reference measurements are done skipping (1), so with the same start/trigger position as with the plate.

3 Discussion of the measuring results

In this chapter the results of the experiments are presented and the observations are discussed. Each experiment is discussed in a separate section.

3.1 Effective rolling radius

First an overview of the unloaded tire radii is depicted in Table 3.1. The unloaded radius (r_f) is determined out of the circumference of the tire, defined by:

$$circumference\ tire = 2\pi r_f \tag{3.1}$$

Code	Tire	Unloaded radius [mm]
GE	Goodyear Eagle NCT5 EMT	317
BT	Bridgestone Turanza RFT	319
DS	Dunlop SP Sport 2000*E	314
MP	Michelin Pilot HX	318

Table 3.1, *Unloaded tire radius*

No significant differences between unloaded radii of the different tires exist, except for the Dunlop tire. The Dunlop has other tire dimensions, which obviously causes an unloaded radius that is slightly lower.

The effective rolling radius is determined according to the measurement procedure described in Section 2.4. Table 3.2 gives an overview of the measured effective rolling radii at the different vertical loads.

	Effective rolling radius [mm]			
Vertical load [kN]	GE	BT	DS	MP
1	311	312	309	311
2	309	311	307	308
3	309	311	306	308
4	308	310	306	307
5	308	310	305	306
6	308	310	305	305

Table 3.2, *Effective rolling radius*

In Fig. 3.1 a graphical representation of the effective rolling radius is given.

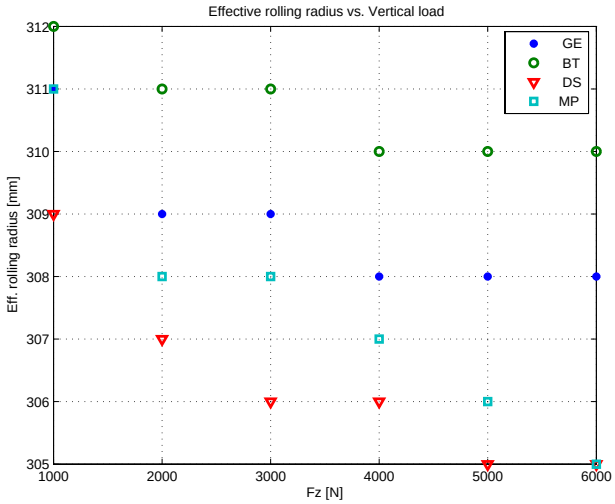

Fig. 3.1, *Effective rolling radius*

Observation of the results shows that the difference between the effective rolling radius of run flat tires and conventional tires is minimal.

3.2 Stiffness measurements

In this section the vertical and lateral stiffness of the different tires will be presented and discussed. Furthermore the lateral friction coefficients, which are determined from the lateral stiffness experiments, are presented.

3.2.1 Vertical stiffness

As described in Section 2.4.1 the vertical stiffness is measured for both the rolling and non-rolling situation. The rolling situation is most common and therefore discussed in this section. The results of the static situation are presented in Appendix 2. The vertical stiffness is determined by obtaining the best polynomial fit[I] through the measured data using Matlab. The results for the rolling situation are depicted in Fig. 3.2.

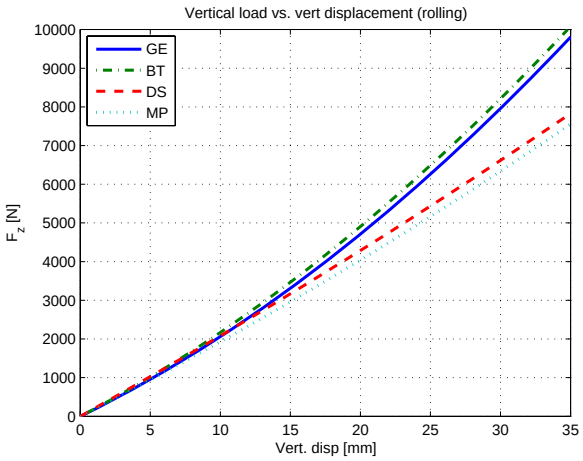

Fig. 3.2, *Comparison vertical stiffness tires (rolling situation)*

Observation of the result shows that run flat tires exhibit a strong nonlinear behavior. Till a vertical load of approximately 3 kN the vertical stiffness of run flat tires not substantially differs from conventional tires. Above a vertical load of 3 kN the vertical stiffness of a run flat tire progressively increases compared to a conventional tire. Note that, the codes GE and BT represent the run flat tires.

Comparison of the run flat tires with the conventional Michelin tire (MP) at a vertical load of 9 kN, shows that the vertical stiffness increases with approximately 45 percent. For the same vertical load the vertical stiffness of the run flat tires increases with 50 percent compared to the conventional Dunlop tire (DS).

[I] See Appendix 2 for polynomial fits of separate tires and corresponding vertical stiffness values

3.2.2 Lateral stiffness

The lateral stiffness is measured according to the procedure described in Section 2.4.2. In Fig. 3.3, the results are depicted for the different tires separately.

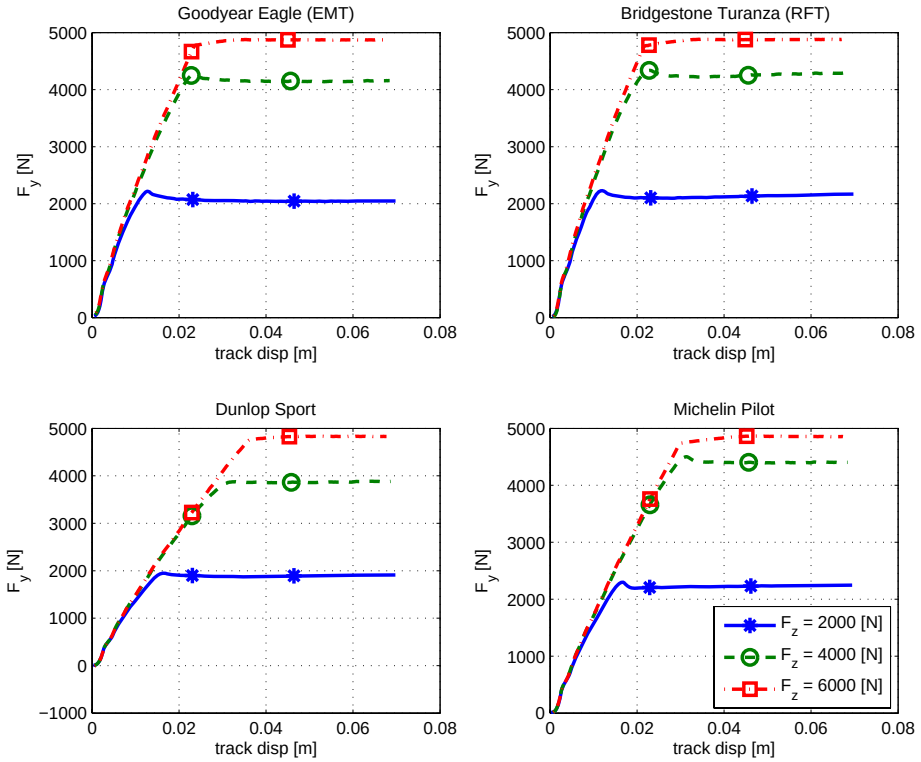

Fig. 3.3, *Lateral force vs. lateral displacement*

Out of the linear sections of the presented results in Fig. 3.2 the lateral stiffness is determined. The lateral stiffness is determined for the different vertical loads. Furthermore the average lateral stiffness is determined out of the three vertical load cases. In table 3.3 an overview of the lateral stiffness is given.

	Lateral stiffness [N/m]			
Vertical load [kN]	**GE**	**BT**	**DS**	**MP**
2	213500	227000	142000	163000
4	216000	232000	144000	167500
6	219000	235000	146000	169000
average	216000	231000	144000	166500

Table 3.3, *Lateral stiffness*

Observations of the results show that run flat tires have a significantly higher lateral stiffness. The stiffness of run flat tires is on average 45 percent higher.

Lateral friction coefficient

Using the results of the lateral stiffness measurements it is possible to determine the lateral friction coefficient of the different tires. The lateral friction coefficient (μ) is defined by the ratio between the steady state lateral force ($F_{y,ss}$) and the vertical load (F_z). Note that the sideslip angle is 90 degrees in this case.

$$\mu = \frac{F_{y,ss}}{F_z} \tag{3.2}$$

Fig. 3.4 gives an overview of the lateral friction coefficient as a function of the vertical load.

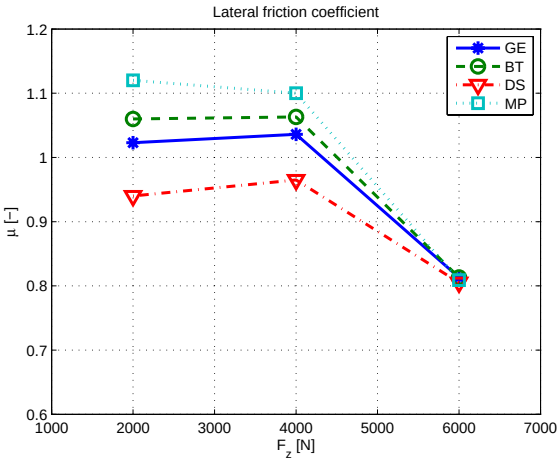

Fig. 3.4, *Lateral friction coefficient*

The markers in Fig. 3.3 show the points where the lateral friction coefficient actually is determined. Observations show that by rising vertical load the friction coefficient of the different tires come close to each other. From a vertical load of 4 kN the friction coefficient decreases. The run flat tires differ not much from each other unlike to the conventional tires.

The results show a different trend as expected. It might be expected that a tire with wider tire dimensions (like the Dunlop tire) has a higher lateral friction coefficient as a smaller tire. Furthermore it might be expected that the lateral friction coefficient decreases at increasing vertical load. But the results in Fig. 3.3 do not show this behaviour. The low sliding speed of the Tire Flat Plank can be the cause of the unexpected results. For instance, on the Tire Test Truck these experiments are performed with a speed of 60 km/h. The results at low sliding velocity differ from results at higher speeds. Also the use of brand-new tires can affect the results. The top layer of the tire tread of brand-new tires is a bit slippery compared to a used tire where this top layer has disappeared.

3.3 Sideslip relaxation

Fig. 3.5 represents the sideslip relaxation behavior of the different tires.

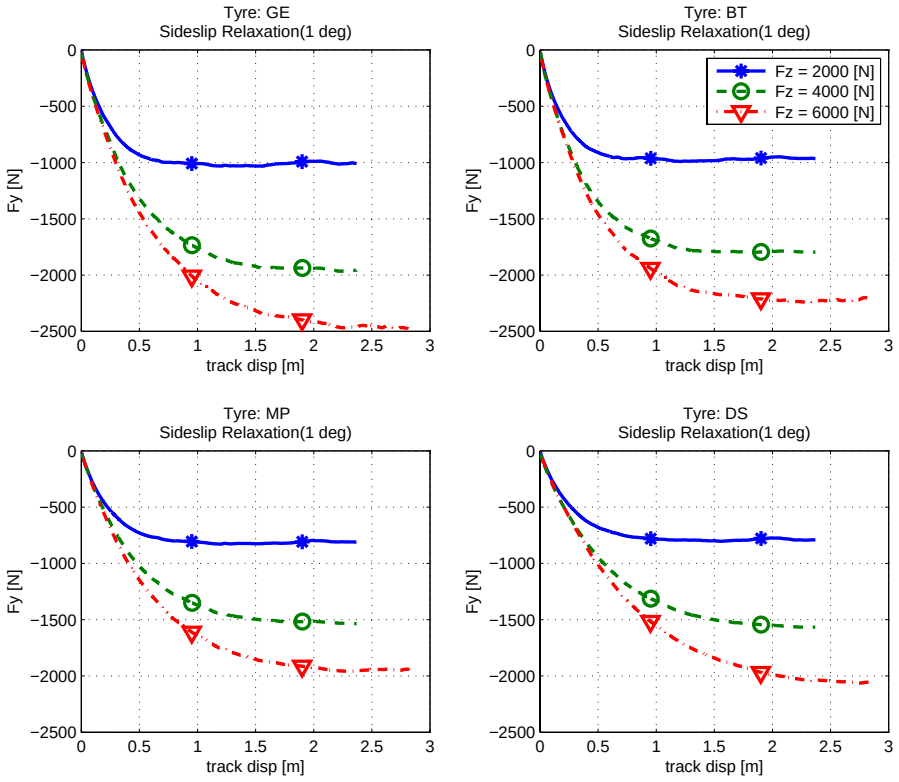

Fig. 3.5, *Sideslip relaxation*

In general, the sideslip relaxation length is defined as the length that corresponds with 63 percent of the steady-state lateral force level.

Observations show that there is no significant difference between the sideslip relaxation behavior of run flat tires and conventional tires. However, run flat tires show a higher level in lateral force steady state value. This is probably the result of the higher lateral stiffness of the tires.

Finally an estimate of the cornering stiffness is given in Table 3.4.

	Cornering stiffness [N/rad]			
Vertical load [kN]	**GE**	**BT**	**DS**	**MP**
2	59000	56000	46000	47000
4	112000	102500	89000	88000
6	140000	127000	118000	111000

Table 3.4, *Cornering stiffness*

The relaxation behavior of the run flat and conventional tires is not very different due to the relation between the cornering and lateral stiffnesses. As described by Pacejka [1], the tire relaxation can be obtained by:

$$\sigma = \frac{C_{F\alpha}}{C_{Fy}} \tag{3.3}$$

where ($C_{F\alpha}$) is the cornering stiffness of the tire and (C_{Fy}) the total lateral stiffness. For run flat tires both stiffnesses are higher with as result that the relaxation length (σ) corresponds rather well with the relaxation length of conventional tires. In Table 3.5 an estimate of the relaxation length is given. The results show that the relaxation length is quite similar for the different tires. Only the Dunlop (conventional) tire differs a bit. This is probably due to the different tire dimensions.

	Relaxation length [m]			
Vertical load [kN]	**GE**	**BT**	**DS**	**MP**
2	0.28	0.25	0.32	0.29
4	0.52	0.44	0.62	0.53
6	0.64	0.55	0.81	0.66

Table 3.5, *Relaxation length*

3.4 Enveloping behavior

In this chapter the results of the cleat measurements, according to Section 2.6, will be discussed. Because of the limited time, the measurements are carried out only for the Goodyear Eagle (RFT) and the Michelin Pilot (conventional tire). First the results of the step obstacle will be discussed, after that the results of the sine obstacle.

3.4.1 Step obstacle

The results of the cleat measurements with the step obstacles are post-processed and expressed in two characterizing variables, namely the effective height (w) and the effective forward slope (β_y). Both variables are defined in one point: the wheel centre, and are used to describe the so-called effective road plane. The position and orientation of the two-dimensional effective road plane is defined such that the resulting force that acts upon the wheel axle is directed perpendicularly to the effective road plane [3], see Fig. 3.6. Assumed is that the friction may be neglected.

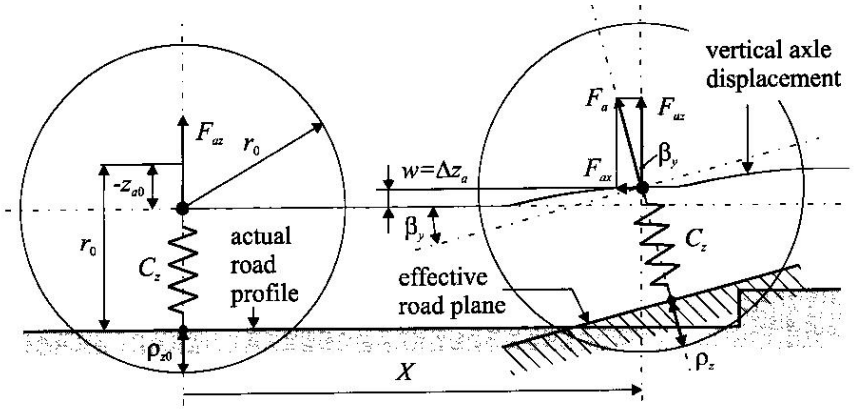

Fig. 3.6, *The wheel rolled over an obstacle at constant vertical load to establish the two-dimensional effective road surface. The spindle force (Fa) acts from the tyre on the wheel axle. [3]*

The effective height (w) is defined as the distance over which the wheel centre has to move vertically in order to keep the vertical load constant when rolling over an obstacle:

$$w = dz \tag{3.4}$$

Here (dz) is vertical axle displacement of the Tire Flat Plank to keep the vertical load constant. For compensating the small variations of the vertical load that cannot be compensated by the air spring system of the Tire Flat Plank, a correction factor (w_c) is introduced:

$$w = dz + w_c \tag{3.5}$$

The correction factor (w_c) is defined as followed:

$$w_c = \frac{F_{az} - F_{az0}}{C_{Fz}} \tag{3.6}$$

The effective forward slope (β_y) is defined as the longitudinal spindle force (F_{ax}) divided by the constant vertical spindle force (F_{az}):

$$\tan \beta_y = \frac{F_{ax}}{F_{az}} \tag{3.7}$$

The following equations apply:

$$F_{ax} = F_a \sin \beta_y \tag{3.8}$$

$$F_{az} = F_a \cos \beta_y \tag{3.9}$$

Fig. 3.7 – Fig. 3.9 represent the results of the step obstacle measurements. The figures show the results of respectively 10, 20 and 30 mm obstacle height.

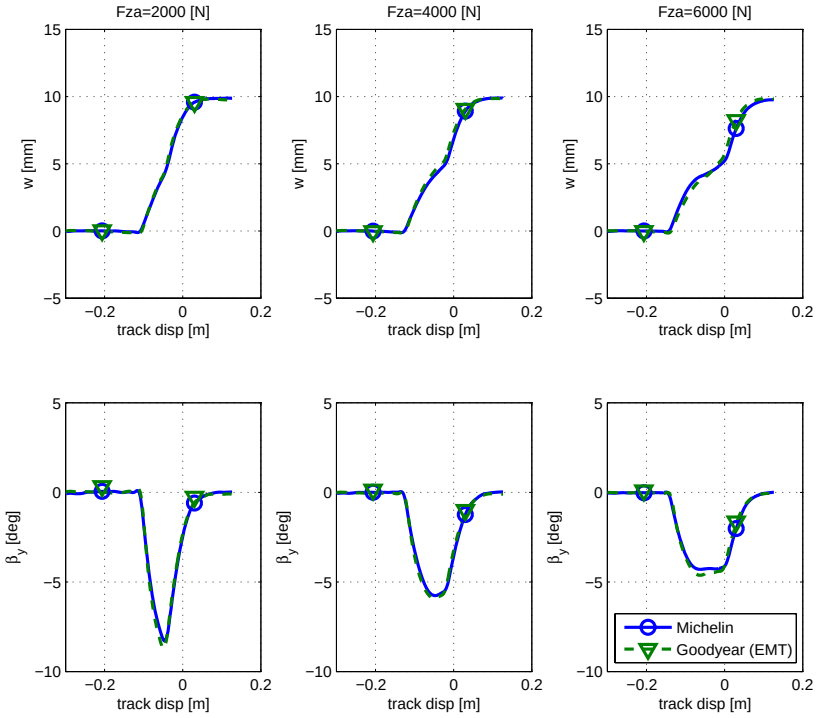

Fig. 3.7, *Response at step obstacle (10 mm)*

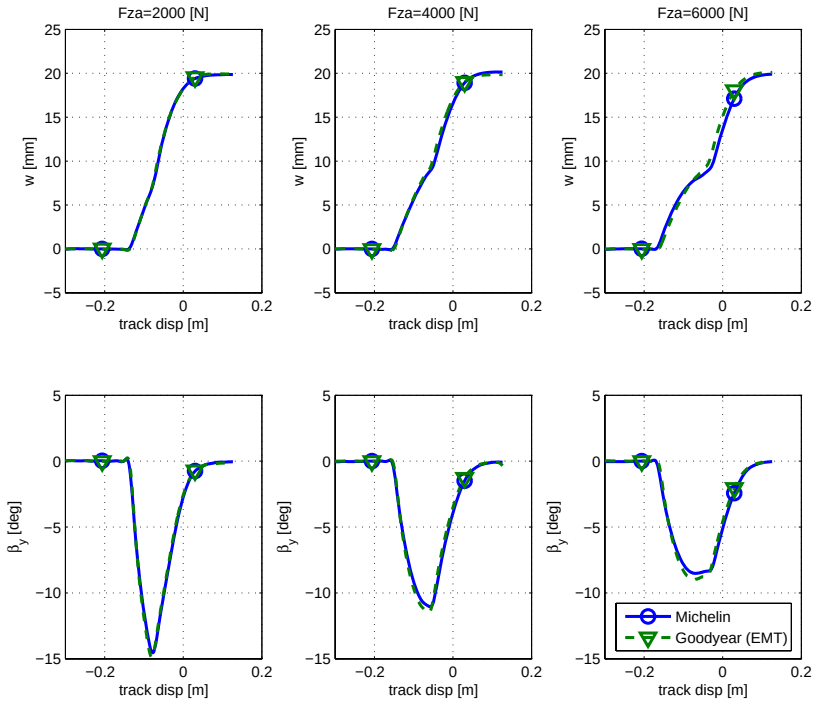

Fig. 3.8, *Response at step obstacle (20 mm)*

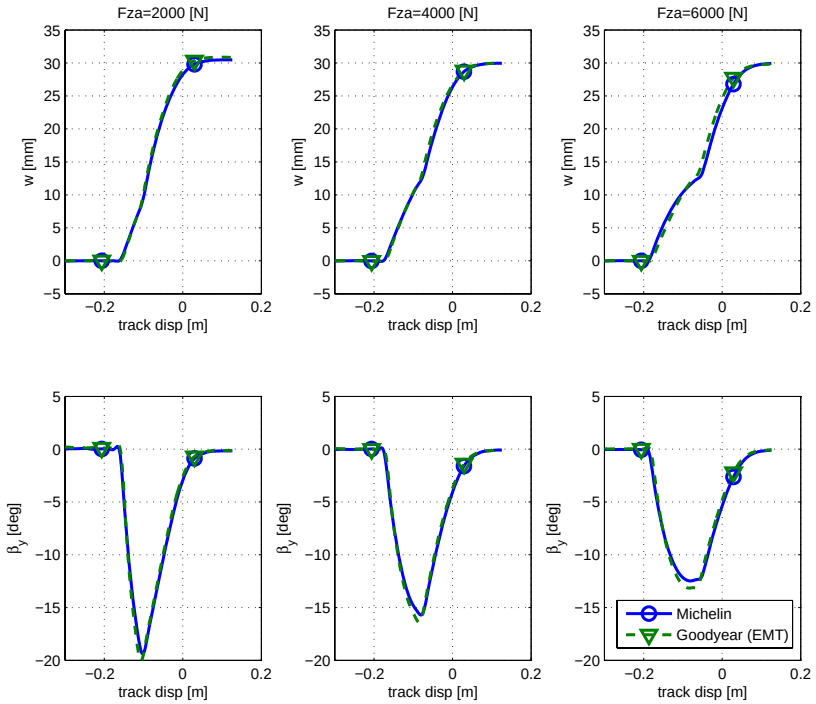

Fig. 3.9, *Response at step obstacle (30 mm)*

Observations of the results show that there is no significant difference between the run flat tire and the conventional tire. The effective slope (β_y) and the effective height (w) are for both tires about the same. At higher obstacle heights a slight difference between the tires arises. In Fig. 3.7 – 3.9, it can be observed that the point of first contact with the obstacle is the same for both tires. This equal enveloping behavior would indicate that the tire outside contour and contact length of both tires is very similar. Fig. 3.10 illustrates the point of first contact of a tire with an obstacle, (l_s) is the contact length. In Appendix 3 an overview of the contact length for different vertical loads and the footprints of the contact patches for different vertical loads are presented. As can be seen in this Appendix the contact lengths for the various tires do not differ much for a specific vertical load.

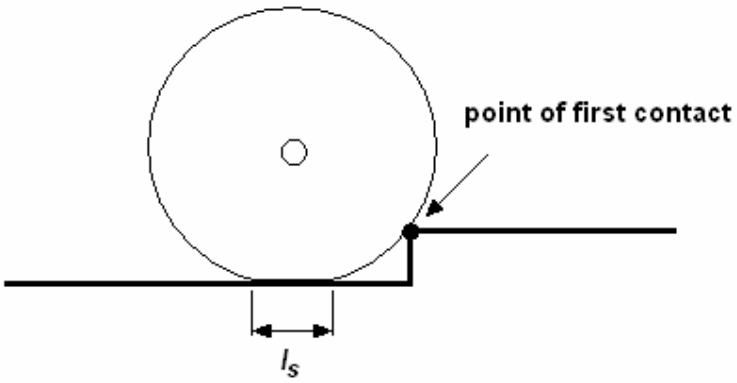

Fig. 3.10, *Point of first contact with an obstacle*

3.4.2 Sine obstacle

As described before, the sine obstacle measurements are carried out with constant axle height (see Section 2.6.2). The results of the measurements are represented in the change of vertical load (ΔF_z) and the change of longitudinal force (ΔF_x). In fig. 3.9 the results for the different vertical loads are depicted.

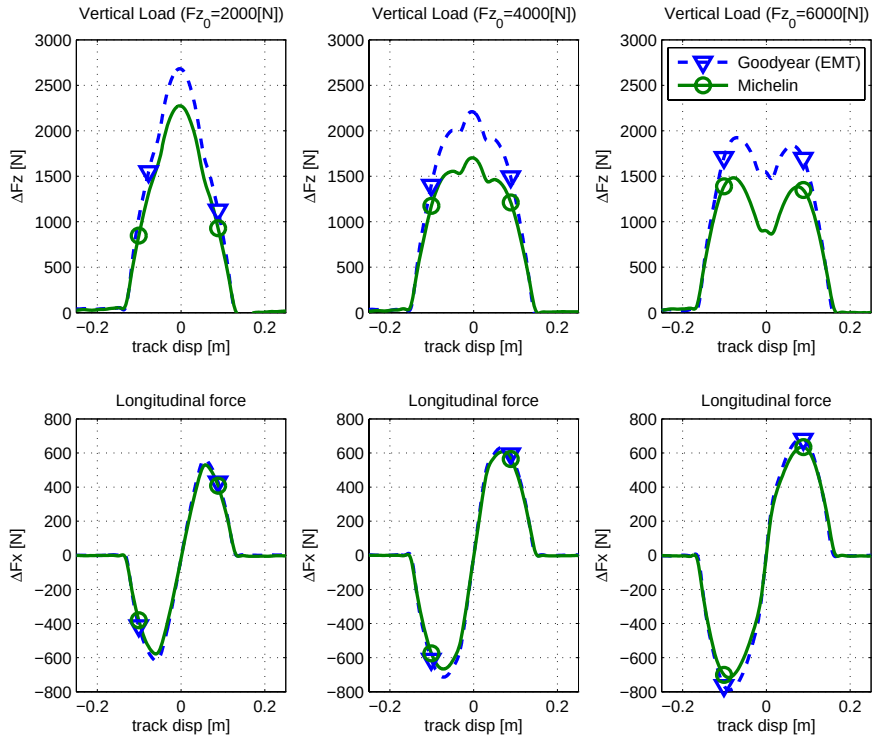

Fig. 3.9, *Response at sine obstacle*

Observation of the results shows that the vertical load of the run flat tire increases more in comparison to the conventional tire. The higher increase in vertical load is the result of the higher vertical stiffness of the run flat tire. The moment, i.e. position, of increase in vertical load is for both tires the same, which again would indicate that the tire outside contour and contact length of both tires is probably very similar (see Appendix 3). Further observations show that there is no significant difference in longitudinal force change between the run flat tire and the conventional tire.

4 Conclusions and Recommendations

This Chapter presents the main conclusions of this project. In addition, some recommendations for further research are formulated. The subject of this research project was the study of the differences in characteristics of conventional tires and Run Flat Tires. The aims of this research were: (1) examination of the characterizations of conventional tires and Run Flat Tires and (2) understanding the differences in characterizations between conventional tires and Run Flat Tires. To achieve these aims, a number of experiments were carried out on the Tire Flat Plank and analyzed to create a better perception of the characterization differences. This report deals with the outcome of these experiments and describes the differences in characterizations.

4.1 Conclusions

The following conclusions have been drawn with respect to characterizations differences of conventional tires and run flat tires:

Stiffness

- Till a vertical load of 3 kN, the vertical stiffness of run flat tires is about the same as of conventional tires.
- Above a vertical load of 3 kN, the vertical stiffness of run flat tires increases significantly more progressively.
- The lateral stiffness of run flat tires is considerably higher than that of conventional tires. The difference can increase up to 50 percent higher.

Sideslip relaxation

- The relaxation lengths of run flat tires and conventional tires do not significantly differ.
- Run flat tires show a higher steady state lateral force level. This is related to the higher lateral stiffness of run flat tires.

Enveloping behavior

- At constant vertical load, both tires show the same behavior at step obstacles. This can be explained by the fact that the contact patch length and the outside contour of the considered run flat tire (Goodyear) and the considered conventional tire (Michelin) are approximately the same. When rolling with constant axle height over a sine cleat, the point of first contact with the cleat is also the same for both tires.
- When rolling over a sine obstacle with constant axle height, the considered run flat tire (Goodyear) shows more increase in vertical load than the conventional tire (Michelin). This is related to the higher vertical stiffness of the run flat tire.

Finally, when the aims of the research project that are formulated in Chapter 1 are considered, it can be assessed to what extent these aims have been achieved. These aims were: (1) examining the characterizations of conventional tires and Run Flat Tires and (2) understanding the differences in characterizations between conventional tires and Run Flat Tires. For these aims, the following characterization areas are examined: (i) the effective rolling radius, (ii) the lateral and vertical stiffness, (iii) the sideslip relaxation and (iv) the enveloping behavior. Considering all these aims and experiments performed, it is concluded that all aims formulated at the beginning of this research project are achieved in a satisfying way, although several topics will require further investigations. These

topics are listed in the next section where recommendations for further research are formulated

4.2 Recommendations

The following recommendations can be done for further research:

- Although in this project the stiffnesses were considered, there were no experiments carried out to determine the longitudinal stiffness of the tires. In future research it is interesting to investigate the longitudinal stiffness and to see if there are differences between run flat and conventional tires.

- Due to limited time, the cleat measurements to investigate the enveloping behavior were determined only for one run flat tire (Goodyear) and one conventional tire (Michelin). In further research it is recommended to do the same cleat measurements for the other run flat (Bridgestone) and conventional tire (Dunlop) to create a wider view of the differences in enveloping behavior.

- Carry out additional measurements to completely characterize the run flat tires. For further research this would mean: principal tire modes, damping ratios, slip characteristics, vertical stiffness at various velocities, etc.

- When a vehicle drives over an uneven road surface the axle height is not constant and also the vertical load is not constant. Therefore, to investigate the differences between run flat and conventional tires, vehicle simulations and measurements have to be carried out on various road surfaces.

References

[1] Pacejka, H.B.(2002), *Tyre and Vehicle Dynamics*, Butterworth-Heinemann, An imprint of Elsevier Science, ISBN 0-7506-5141-5, www.bh.com, 2002

[2] Higuchi, A. (1997), *Transient Response of Tires at Large Wheel Slip and Camber*, PhD Thesis, Delft University of Technology, Delft, The Netherlands, ISBN 90-407-1563-7, 1997

[3] Schmeitz, A.J.C. (2004), *A Semi-Empirical Three-Dimensional Model of the Pneumatic Tire Rolling over Arbitrarily Uneven Road Surfaces*, PhD Thesis, Delft University of Technology, Delft, The Netherlands, ISBN 90-9018380-9, 2004

[4] Tire tech, *Run Flat Tires,* www.tirerack.com/tires/tiretech/techpage.jsp?techid=56

[5] Martini, M. (2005), *A Run-Flat Future*, SAE100 Future Look article, april 2005

[6] Tires online, Tyre technology: *Goodyear EMT Runflat Technology*, www.tyres-online.co.uk/technology/emt.asp

Appendix 1 Forces and moments transformation

Fig. A1.1 depicts the measuring hub. The measuring hub can measure reaction forces (up to 10 kN) and moments by using strain gauge bridges. The strain gauge bridges sense the longitudinal forces G_{x1} and G_{x2}, the lateral force G_y and the vertical forces G_{z1} and G_{z2}. To calculate the moments at wheel axle the distance (a) between the forces G_{x1} and G_{x2} and the distance (b) between G_{x2} and the wheel centre plane are used.

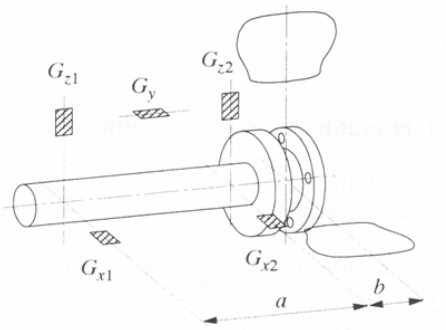

Fig. A1.1, *Measuring hub [2]*

The forces and moments at the wheel axle are defined as follows:

$$K_x = G_{x1} + G_{x2} \quad \text{(A1.1)}$$

$$K_y = G_y \quad \text{(A1.2)}$$

$$K_z = G_{z1} + G_{z2} \quad \text{(A1.3)}$$

$$T_x = G_{z1}(a+b) + G_{z2}b \quad \text{(A1.4)}$$

$$T_y = 0 \quad \text{(A1.5)}$$

$$T_z = G_{x1}(a+b) + G_{x2}b \quad \text{(A1.6)}$$

The coordinate system of the measuring hub and at the contact centre is depicted in Fig. A1.2.

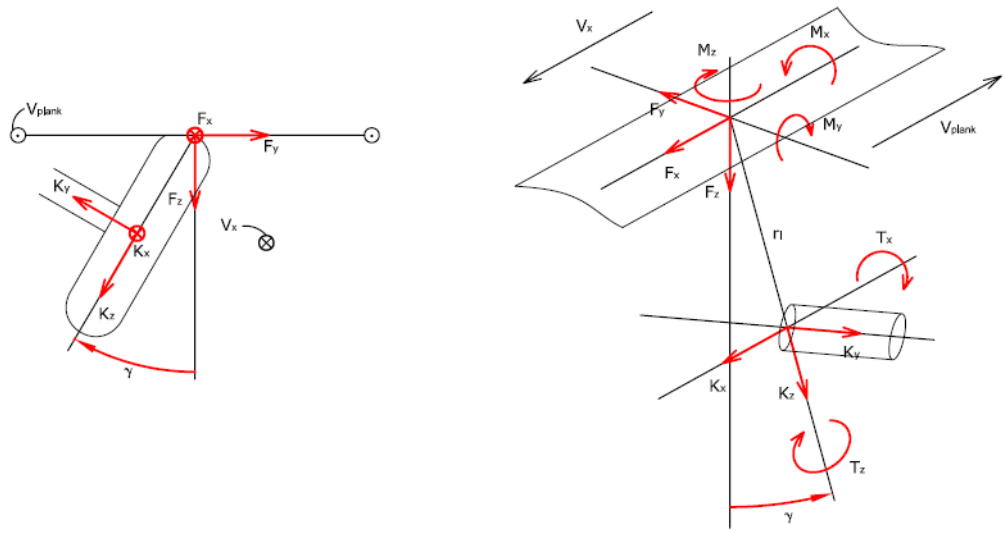

Fig. A1.2, *Coordinate system measuring hub and contact centre*

The forces and moments measured at the measuring hub are transformed to forces and moments at the contact centre (ISO coordinate system). According to Fig. A1.2, the transformations are as follows:

$$F_x = K_x \tag{A1.7}$$

$$F_y = -K_y \cos\gamma - K_z \sin\gamma \tag{A1.8}$$

$$F_z = -K_y \sin\gamma + K_z \cos\gamma \tag{A1.9}$$

$$M_x = -T_x + K_y r_l \tag{A1.10}$$

$$M_y = -T_z \sin\gamma + K_x r_l \cos\gamma \tag{A1.11}$$

$$M_z = T_z \cos\gamma + K_x r_l \sin\gamma \tag{A1.12}$$

Note that (r_l) is the loaded radius and consequently is a positive number in these equations.

Appendix 2 Vertical stiffness

As described in Section 2.4.1, the vertical stiffness measurements are carried out for both a rolling and static (stand still) situation. The rolling situation is discussed in Section 3.2.1. This Section contains the non-rolling situation and the polynomial fits of separate tires with corresponding vertical stiffness values.

A2.1 Vertical stiffness (non-rolling situation)

The results for the static situation are depicted in Fig. A2.1. Presented are the polynomial fits of the different tires.

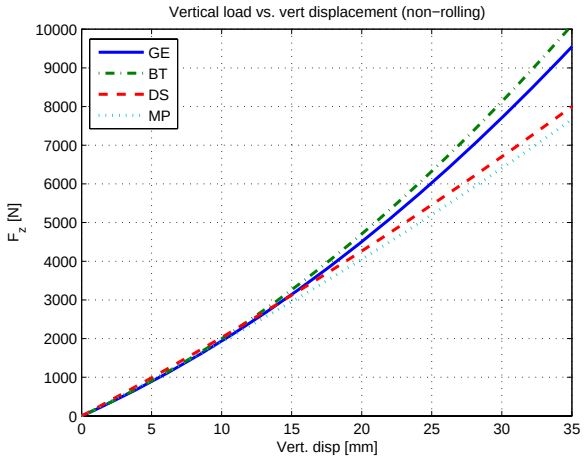

Fig. A2.1, *Comparison vertical stiffness tires (static situation)*

Observations show that the same conclusions can be drawn as for the rolling situation (see Section 3.2.1). Up to approximately 2.5 kN vertical load, the vertical stiffness of the run flat tires does not substantially differ from the conventional tires. Above this vertical load, the vertical stiffness of the run flat tires progressively increases much more compared to the conventional tires.

A2.2 Vertical stiffness polynomial fits

In this section the polynomial fits of the different tires are presented for both the rolling and the static situation. Also the polynomial fit equations, the linear vertical stiffness equations and the corresponding values are given.

The polynomial fit used is a quadratic fit. First a quadratic fit is determined for the three measurements separately. Then the final fit is derived out of the average of the three separate quadratic fits. The vertical stiffness equation is derived out of the final fit equation. This is the tangent in a specific point of the quadratic fit. The resulting vertical stiffness is presented for the following vertical loads: 2, 4, 6 and 9 kN. In the figures mentioned below, the measurement data is presented as a thin line and the quadratic fit as a thick line.

In Fig. A2.2 the results of the Goodyear Eagle EMT are depicted.

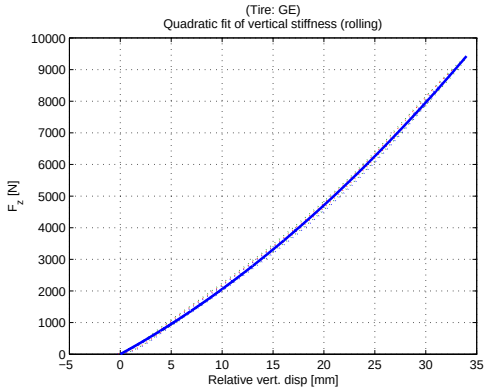

$$fit\ equation:\ F_z = 2.9707 d_z^2 + 176.21 d_z$$

$$stiffness\ equation:\ C_z = \frac{dF_z}{dd_z} = 5.9414 d_z + 176.21$$

$$F_z = 2[kN]\ ,\ d_z = 9.75[mm] \ \Rightarrow\ C_z = 2.34 \cdot 10^5 [N/m]$$
$$F_z = 4[kN]\ ,\ d_z = 17.52[mm] \ \Rightarrow\ C_z = 2.80 \cdot 10^5 [N/m]$$
$$F_z = 6[kN]\ ,\ d_z = 24.19[mm] \ \Rightarrow\ C_z = 3.20 \cdot 10^5 [N/m]$$
$$F_z = 9[kN]\ ,\ d_z = 32.87[mm] \ \Rightarrow\ C_z = 3.72 \cdot 10^5 [N/m]$$

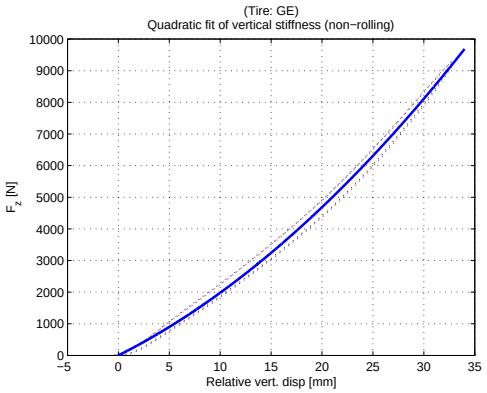

$$fit\ equation:\ F_z = 3.6167 d_z^2 + 161.94 d_z$$

$$stiffness\ equation:\ C_z = \frac{dF_z}{dd_z} = 7.2334 d_z + 161.94$$

$$F_z = 2[kN]\ ,\ d_z = 10.08[mm] \ \Rightarrow\ C_z = 2.35 \cdot 10^5 [N/m]$$
$$F_z = 4[kN]\ ,\ d_z = 17.70[mm] \ \Rightarrow\ C_z = 2.93 \cdot 10^5 [N/m]$$
$$F_z = 6[kN]\ ,\ d_z = 24.09[mm] \ \Rightarrow\ C_z = 3.36 \cdot 10^5 [N/m]$$
$$F_z = 9[kN]\ ,\ d_z = 32.29[mm] \ \Rightarrow\ C_z = 3.96 \cdot 10^5 [N/m]$$

Fig. A2.2, *Measurements (thin) and quadratic fit (thick) Goodyear Eagle EMT*

In Fig. A2.3 the results of the Bridgestone Turanza RFT are depicted.

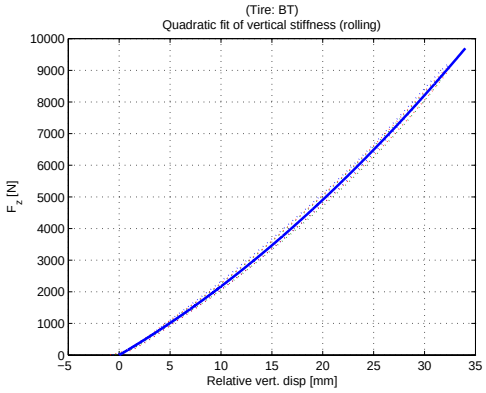

$$fit\ equation:\ F_z = 2.8423 d_z^2 + 188.52 d_z$$

$$stiffness\ equation:\ C_z = \frac{dF_z}{dd_z} = 5.6846 d_z + 188.52$$

$$F_z = 2[kN]\ ,\ d_z = 9.30[mm] \Rightarrow C_z = 2.41 \cdot 10^5 [N/m]$$
$$F_z = 4[kN]\ ,\ d_z = 16.91[mm] \Rightarrow C_z = 2.85 \cdot 10^5 [N/m]$$
$$F_z = 6[kN]\ ,\ d_z = 23.50[mm] \Rightarrow C_z = 3.22 \cdot 10^5 [N/m]$$
$$F_z = 9[kN]\ ,\ d_z = 32.15[mm] \Rightarrow C_z = 3.71 \cdot 10^5 [N/m]$$

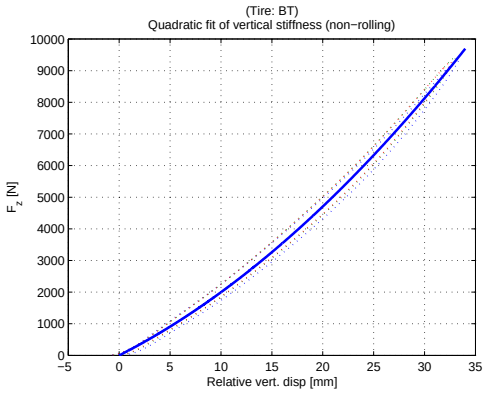

$$fit\ equation:\ F_z = 3.5637 d_z^2 + 163.99 d_z$$

$$stiffness\ equation:\ C_z = \frac{dF_z}{dd_z} = 7.1274 d_z + 163.99$$

$$F_z = 2[kN]\ ,\ d_z = 10.02[mm] \Rightarrow C_z = 2.35 \cdot 10^5 [N/m]$$
$$F_z = 4[kN]\ ,\ d_z = 17.63[mm] \Rightarrow C_z = 2.90 \cdot 10^5 [N/m]$$
$$F_z = 6[kN]\ ,\ d_z = 24.04[mm] \Rightarrow C_z = 3.35 \cdot 10^5 [N/m]$$
$$F_z = 9[kN]\ ,\ d_z = 29.66[mm] \Rightarrow C_z = 3.75 \cdot 10^5 [N/m]$$

Fig. A2.3, *Measurements (thin) and quadratic fit (thick) Bridgestone Turanza RFT*

In Fig. A2.4 the results of the Dunlop SP Sport (conventional) are depicted.

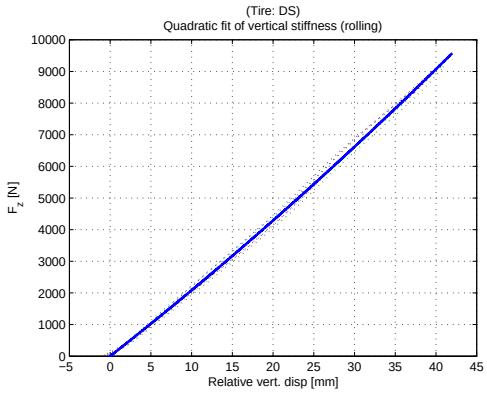

$$fit\ equation:\ F_z = 0.6199 d_z^2 + 201.98 d_z$$

$$stiffness\ equation:\ C_z = \frac{dF_z}{dd_z} = 1.2397 d_z + 201.98$$

$$F_z = 2[kN]\ ,\ d_z = 9.62[mm] \ \Rightarrow\ C_z = 2.14 \cdot 10^5 [N/m]$$
$$F_z = 4[kN]\ ,\ d_z = 18.73[mm] \ \Rightarrow\ C_z = 2.25 \cdot 10^5 [N/m]$$
$$F_z = 6[kN]\ ,\ d_z = 27.40[mm] \ \Rightarrow\ C_z = 2.36 \cdot 10^5 [N/m]$$
$$F_z = 9[kN]\ ,\ d_z = 39.72[mm] \ \Rightarrow\ C_z = 2.51 \cdot 10^5 [N/m]$$

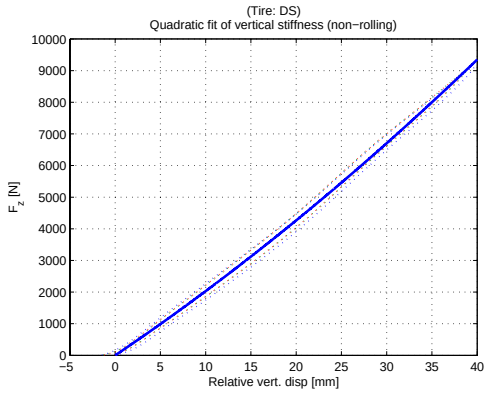

$$fit\ equation:\ F_z = 1.0228 d_z^2 + 192.80 d_z$$

$$stiffness\ equation:\ C_z = \frac{dF_z}{dd_z} = 2.0456 d_z + 192.80$$

$$F_z = 2[kN]\ ,\ d_z = 9.86[mm] \ \Rightarrow\ C_z = 2.13 \cdot 10^5 [N/m]$$
$$F_z = 4[kN]\ ,\ d_z = 18.86[mm] \ \Rightarrow\ C_z = 2.31 \cdot 10^5 [N/m]$$
$$F_z = 6[kN]\ ,\ d_z = 27.20[mm] \ \Rightarrow\ C_z = 2.48 \cdot 10^5 [N/m]$$
$$F_z = 9[kN]\ ,\ d_z = 38.73[mm] \ \Rightarrow\ C_z = 2.72 \cdot 10^5 [N/m]$$

Fig. A2.4, *Measurements (thin) and quadratic fit (thick) Dunlop SP Sport*

In Fig. A2.5 the results of the Michelin Pilot (conventional) are depicted.

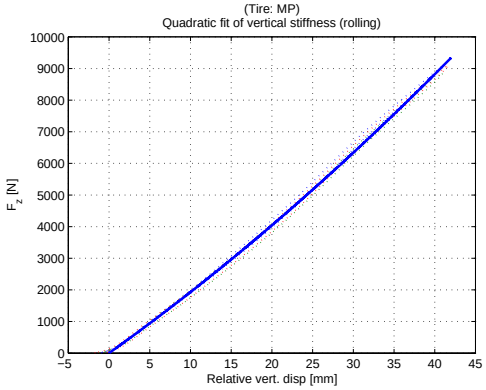

$$fit\ equation:\ F_z = 0.9219 d_z^2 + 183.58 d_z$$

$$stiffness\ equation:\ C_z = \frac{dF_z}{dd_z} = 1.8438 d_z + 183.58$$

$$F_z = 2[kN]\ ,\ d_z = 10.36[mm] \Rightarrow C_z = 2.03 \cdot 10^5 [N/m]$$
$$F_z = 4[kN]\ ,\ d_z = 19.82[mm] \Rightarrow C_z = 2.20 \cdot 10^5 [N/m]$$
$$F_z = 6[kN]\ ,\ d_z = 28.58[mm] \Rightarrow C_z = 2.36 \cdot 10^5 [N/m]$$
$$F_z = 9[kN]\ ,\ d_z = 40.70[mm] \Rightarrow C_z = 2.59 \cdot 10^5 [N/m]$$

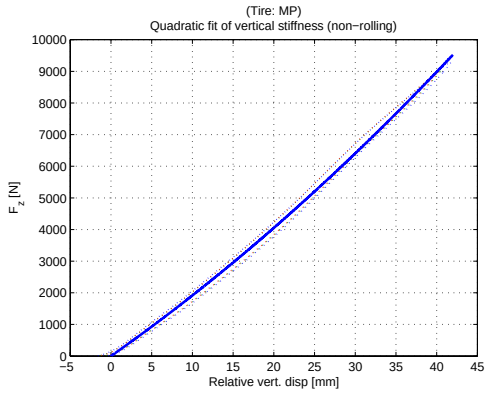

$$fit\ equation:\ F_z = 1.1007 d_z^2 + 180.49 d_z$$

$$stiffness\ equation:\ C_z = \frac{dF_z}{dd_z} = 2.2014 d_z + 180.49$$

$$F_z = 2[kN]\ ,\ d_z = 10.42[mm] \Rightarrow C_z = 2.03 \cdot 10^5 [N/m]$$
$$F_z = 4[kN]\ ,\ d_z = 19.78[mm] \Rightarrow C_z = 2.24 \cdot 10^5 [N/m]$$
$$F_z = 6[kN]\ ,\ d_z = 28.34[mm] \Rightarrow C_z = 2.43 \cdot 10^5 [N/m]$$
$$F_z = 9[kN]\ ,\ d_z = 40.07[mm] \Rightarrow C_z = 2.69 \cdot 10^5 [N/m]$$

Fig. A2.5, *Measurements (thin) and quadratic fit (thick) Michelin Pilot*

Appendix 3 Contact length

In Table A3.1 an overview is given of the estimated tire contact length for several vertical loads. To determine the contact length a footprint of the contact patch is made. The contact length is determined by measuring the length of the footprint.

	Contact length [mm]			
Vertical load [kN]	**GE**	**BT**	**DS**	**MP**
2	92	90	87	89
4	125	130	127	135
6	157	164	167	171

Table A3.1, *Contact length*

In Fig. A3.1 a graphical representation of the contact length for increasing vertical load is given.

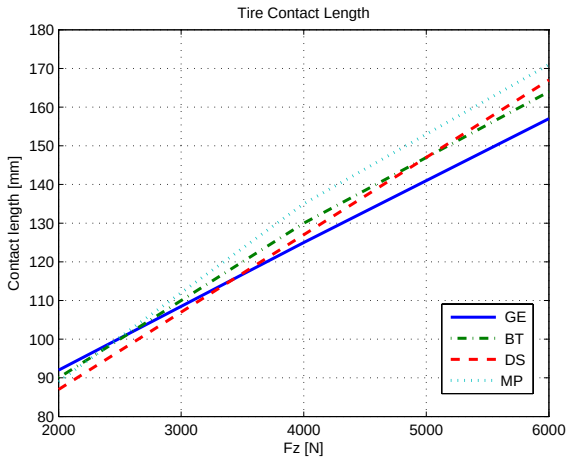

Fig. A3.1, *Contact length at raising vertical loads*

Observation of the results presented in Table A3.1 and Fig. A3.1 shows that the contact lengths do not differ much for the run flat tires and the conventional tires. This corresponds with the conclusions drawn in Section 3.4 with regard to the enveloping behavior.

In Fig. A3.2 – A3.4 the footprints of the contact patches for the different vertical loads are depicted. Notice that all the footprints are scaled with the same scaling factor; dimensions of the depicted footprints are reduced to 15 percent of the actual dimensions.

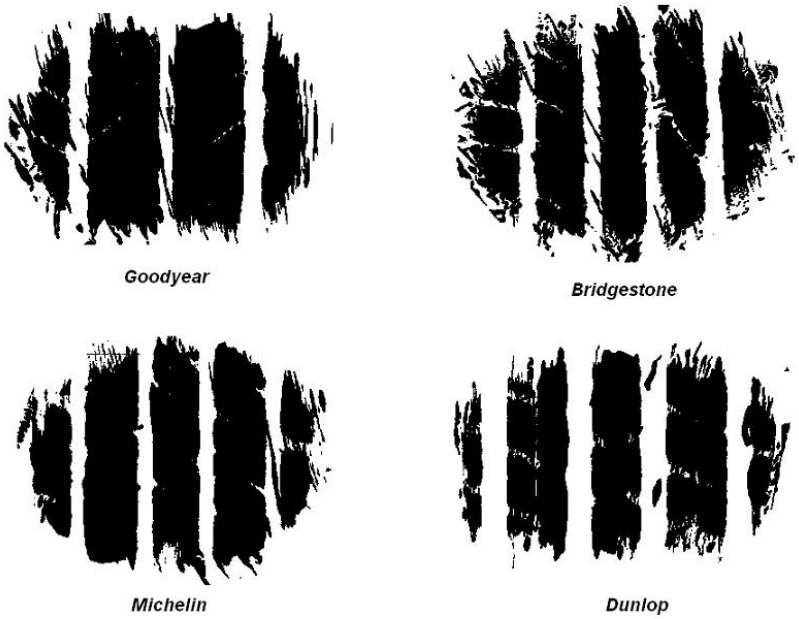

Fig. A3.2, *Footprint contact patch at vertical load 2 kN*

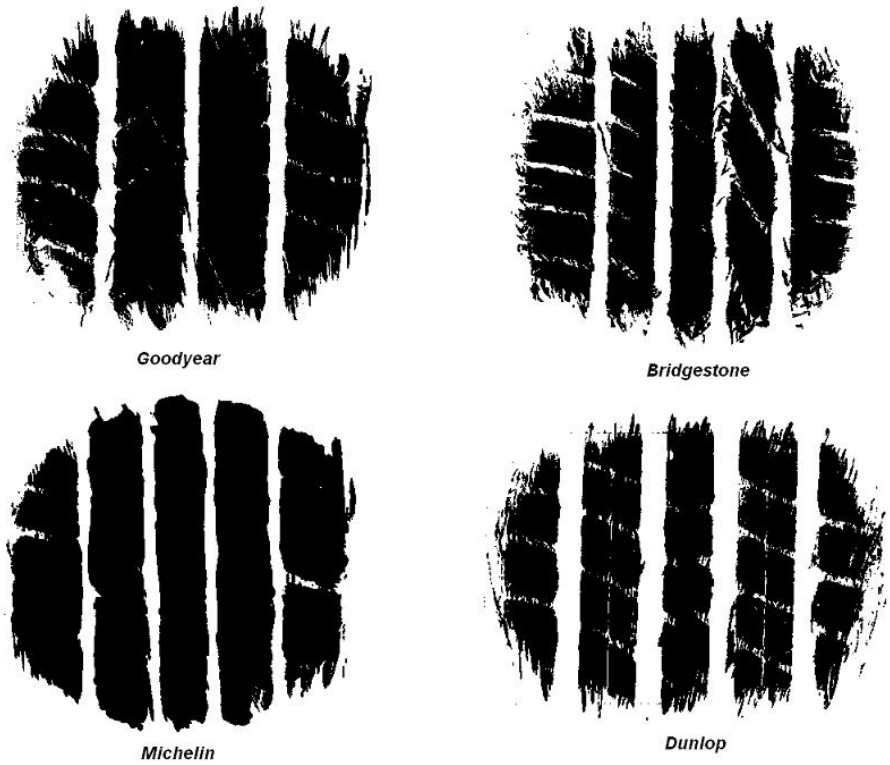

Fig. A3.3, *Footprint contact patch at vertical load 4 kN*

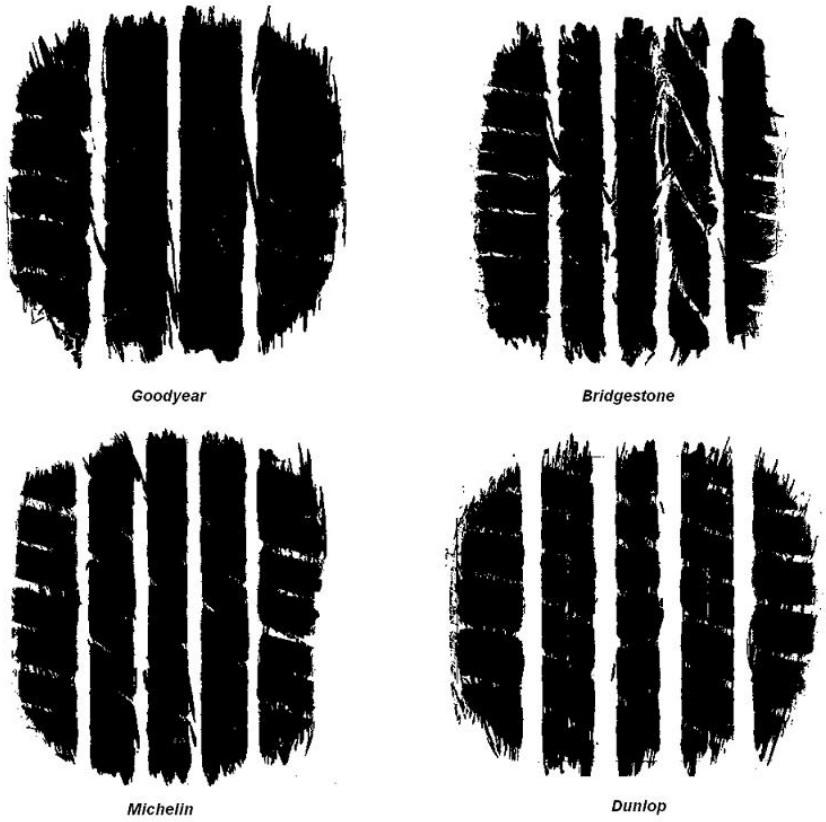

Fig. A3.3, *Footprint contact patch at vertical load 6 kN*

Observation of the footprints shows that the contact patches are quite similar for the run flat tires and the conventional tires. Only the Dunlop tire differs a bit due to other tire dimensions.

Appendix 4 Measurement file name explanation

All the measurements carried out are saved with a unique name containing specific characters to identify the performed experiment, tested tire, vertical load, etc.

Effective rolling radius
The file naming used to save the effective rolling radius measurement data is:
e*ffr_l2000_GE*.
This file naming contains the following specific characters:
- e*ffr* : effective rolling radius experiment
- *l2000* : vertical load (in this case 2000 N)
- *GE* : tested tire (in this case the Goodyear Eagle)

Vertical stiffness
The file naming used to save the vertical stiffness measurement data is:
vertstiffl9000_roll_DS.
This file naming contains the following specific characters:
- *vertstiff* : vertical stiffness experiment
- *l9000* : vertical load (in this case raised till 9000 N)
- *roll* : rolling situation performed (*stat*: non-rolling situation)
- *DS* : tested tire (in this case the Dunlop Sport)

Lateral stiffness
The file naming used to save the lateral stiffness measurement data is:
l*atstiffl2000acGEp1*.
This file naming contains the following specific characters:
- *latstiff* : lateral stiffness experiment
- *l2000* : vertical load (in this case 2000 N)
- *ac* : rolling situation performed (*stat*: non-rolling situation)
- *GE* : tested tire (in this case the Goodyear Eagle)
- *p1* : start measuring position tire

Sideslip relaxation
The file naming used to save the lateral stiffness measurement data is:
rellenl4000a1BTp1.
This file naming contains the following specific characters:
- *rellen* : sideslip relaxation length experiment
- *l4000* : vertical load (in this case 4000 N)
- *a1* : sideslip angle of 1 degree (*a0*: sideslip angle of 0 degree)
- *BT* : tested tire (in this case the Bridgestone Turanza)
- *p1* : start measuring position tire

Cleat measurements
The file naming used to save the step obstacle measurement data is:
cl10l6000lcGEp1.
This file naming contains the following specific characters:
- *cl10* : cleat experiment (in this case 10 mm step height)
- *l6000* : vertical load (in this case 6000 N)
- *lc* : vertical load constant
- *GE* : tested tire
- *p1* : start measuring position tire

The file naming used to save the sine obstacle measurement data is:
clsinl2000acGEp1.
This file naming contains the following specific characters:
- *clsin* : sine cleat experiment
- *l2000* : vertical load (in this case 2000 N)
- *ac* : axle height constant
- *GE* : tested tire
- *p1* : start measuring position tire

Footprint contact patch
The file naming used to save the footprint contact patch measurements is:
fpcpl2000DS.
This file naming contains the following specific characters:
- *fpcp* : Footprint contact patch experiment
- *l2000* : vertical load (in this case 2000 N)
- *DS* : tested tire (in this case the Dunlop Sport)